EGU21-16385

Cascading earthquakes on a fracture network in a geo-reservoir

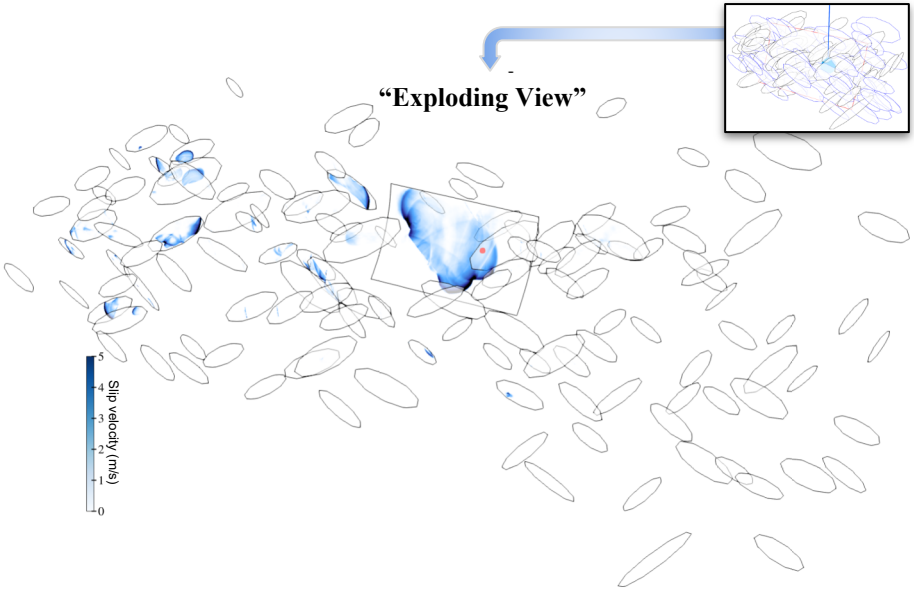

Kadek Hendrawan Palgunadi[1], Alice-Agnes Gabriel[2], Dmitry Garagash[3], Paul Martin Mai[1]

[1]Physical Science and Engineering, King Abdullah University of Science and Technology, Saudi Arabia
[2]Department of Earth and Environmental Sciences, Geophysics, Ludwig-Maximilians-Universitat Munchen, Munich, Germany
[3]Department of Civil and Resource Engineering, Dalhousie University, Halifax, Nova Scotia, Canada

Email: kadek.palgunadi@kaust.edu.sa

Motivation

Illustration of fracture network

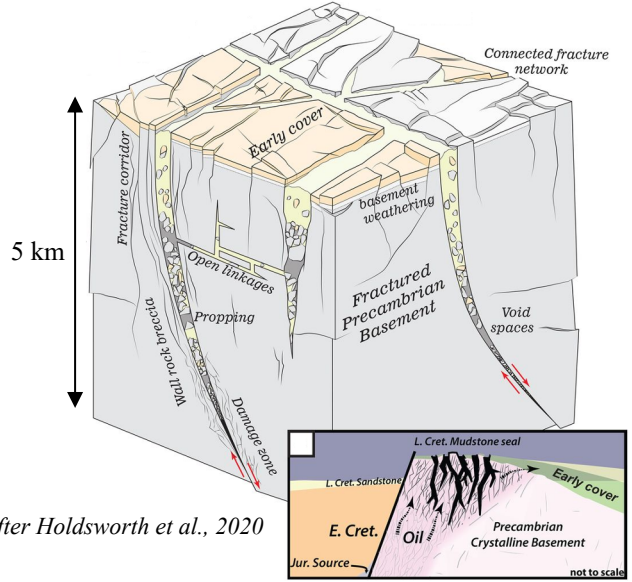

After Holdsworth et al., 2020

Source: http://koreabizwire.com/life-on-hold-for-students-after-pohang-earthquake/101585

- Current understanding on significant induced earthquake (> Mw 4): slip occurs on favorably oriented mapped/unmapped large fault plane with respect to the regional stress loading.
- There might be a possibility for favorably oriented fracture network close to an unfavorable fault plane that produces cascading ruptures.
- Is it possible for dynamic stress interaction among fractures to activate the poorly oriented main fault plane and generate bigger earthquake magnitude?

Motivation

- Non-double couple moment tensor solution on induced event can indicates (Wang et al., 2018; Zhang et al., 2016; Schultz et al., 2020):
    a. tensile fracture growth
    b. multiple intersecting fractures
    c. dilatant jogs created at the overlapping areas of multiple fractures
    d. Non-planar pre-existing fault

Objectives

- Is sustained cascading earthquake rupture possible in fracture network?
- Do such cascading earthquakes require rupture on a “main” fault, or not ?
- Dynamically possible under certain prerequisites: favorable oriented fractures, seismogenic fractures on all scales (scale-dependent co-seismic frictional weakening).
- We only look at one configuration of regional stress loading (S_{hmax} = 65º), assuming (a) fractures being favorably oriented and (b) a main fault misaligned for failure.
- Three different dynamic rupture scenarios:
    - **Scenario 1 (S1): stress/strength perturbation along the main fault only (e.g. injection into a permeable fault core).**
    - **Scenario 2 (S2): stress/strength perturbation into a rock volume spanning a subset of fractures and part of the main fault (e.g. injection into a fracture system within the fault damaged zone).**
    - **Scenario 3 (S3): like S2, but larger stress perturbation.**

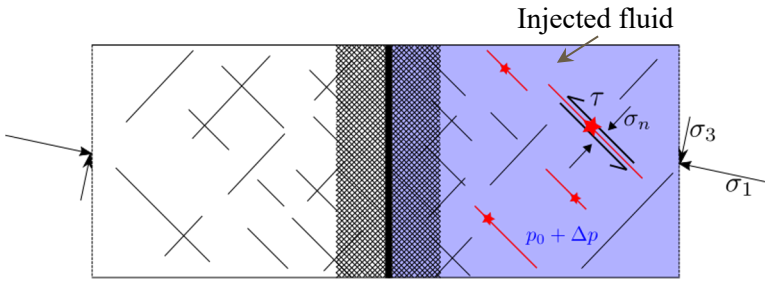

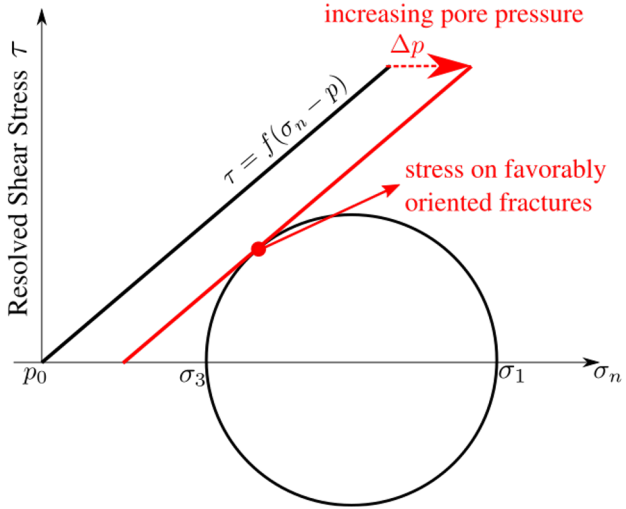

Model of the Fault and Fracture Network

Map view of fracture network

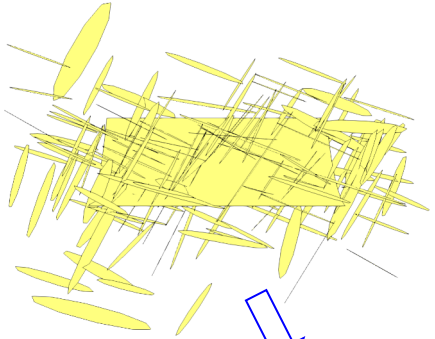

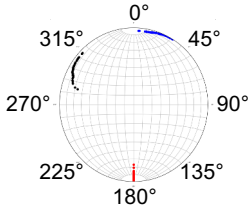

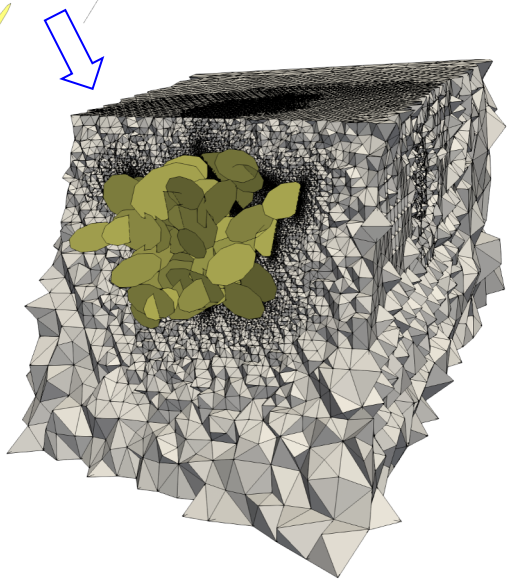

- We follow Savage and Brodsky (2011) to populate fracture density and length distribution.
- Two dominant strike orientations: N20±10 and N120±10, following conjugate off-fault damage from numerical simulations (Okubo et al., 2019; Gabriel et al., 2021) and observation (Mitchell & Faulkner 2009).
- FRACMAN (*Golder Associates Inc.*) software to generate fracture network.
- Elliptic fracture planes.
- We use Simmodeler (*Simmetrix Inc.*) to generate the numerical mesh.
- Mesh grid size is refined toward fault/fracture plane.
- Mesh with 18 mio tetrahedral elements of variable size.
- Fracture plane output from FRACMAN inserted into numerical solver SeisSol (*https://github.com/SeisSol/SeisSol*) to simulate earthquake dynamics and seismic wave propagation.
- The simulation requires approximately 15k core hours for 9 s (simulation time) on Shaheen II, a Cray XC 40 operated by the KAUST Supercomputer Lab.

Fault/fracture scale dependent friction

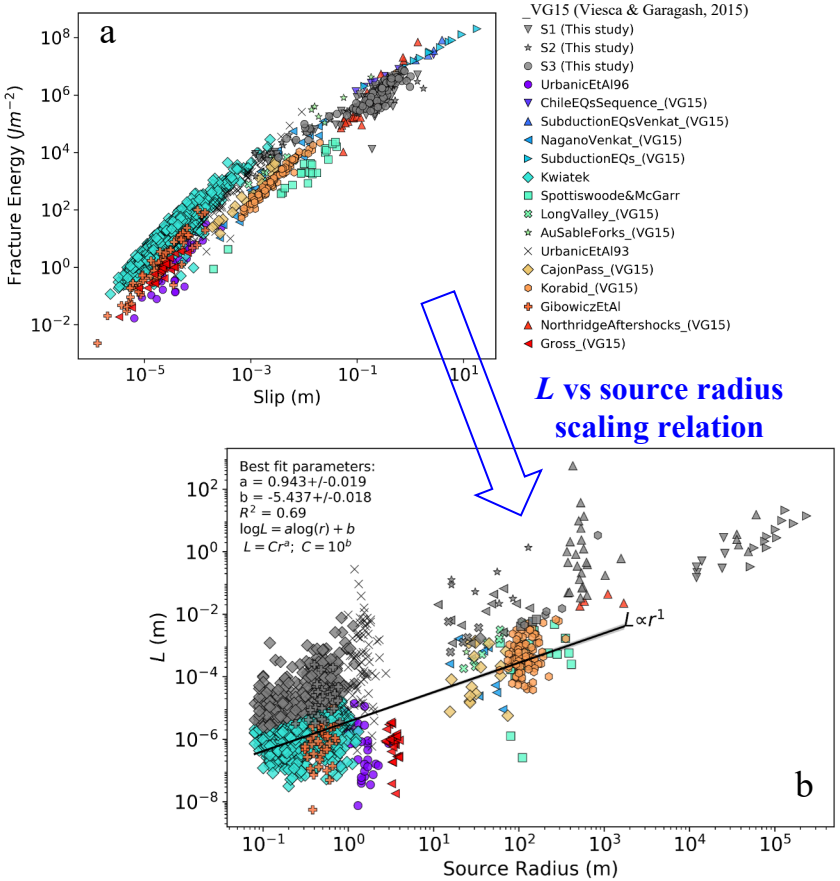

Dependence of *L* on fault/fracture size:

- Fault/fractures are modelled as interfaces with rate-and-state friction characterized by strong rate weakening at coseismic slip rates ('flash heated' friction of Rice (2006), Noda et al. (2009), Dunham et al. (2011).
- Fracture is seismogenic (e.g. can host dynamic slip) if its fault/fracture size (l) exceeds nucleation size that is proportional to L. Hence, L is proportional to l to support co-seismic slip.
- To infer L (Garagash, 2021), we use compilation of fracture energy (G_c) data (Viesca & Garagash, 2015) with additional induced events.

$$L = \frac{G_c}{\Delta f \sigma'},\ \Delta f = f_p - f_w \approx 1,\ \sigma' = \text{effective normal stress}$$

- Assuming l is a representative measure of source radius.
- We use linear fit for scaling relation of L and source radius.
- We can establish threshold of slip → no solution for L due to the assumed friction law (grey symbols in Fig. b; suggesting other weakening mechanism, e.g thermal pressurization (Viesca & Garagash, 2015)).

Optimal Orientation of Fault and Fractures

Original Model

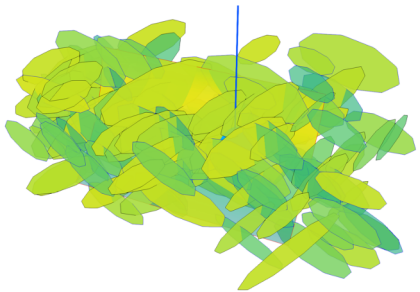

Exploding View

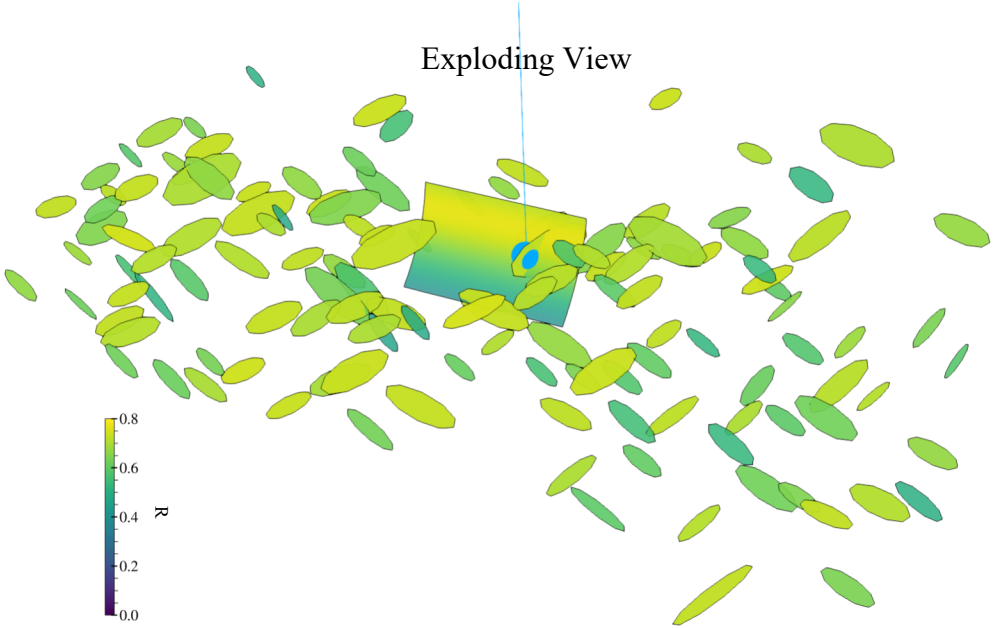

$$R = \frac{\tau_0 - \mu_d \sigma_n'}{(\mu_s - \mu_d)\sigma_n'}$$

- Optimally oriented fractures and non-favourable fault under homogeneous regional stress loading.
- High R-values are more favorable to the regional prestress.
- **Note**: we use constant dynamic and static friction coefficients but varying L with fracture size.

Dynamic Rupture Earthquake Scenario 1

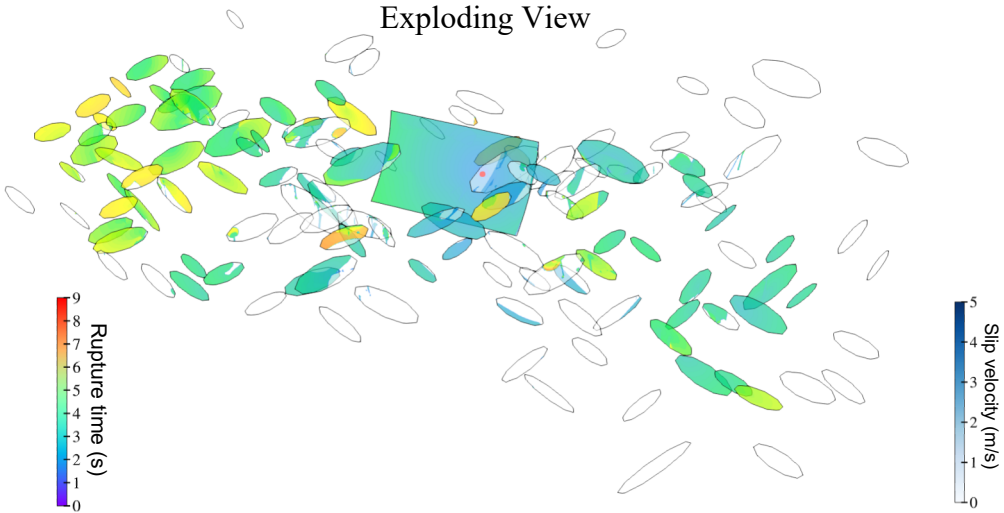

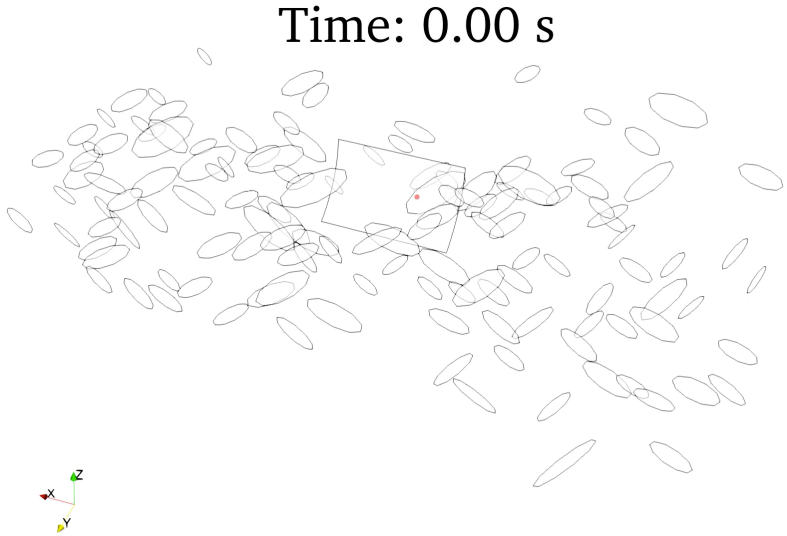

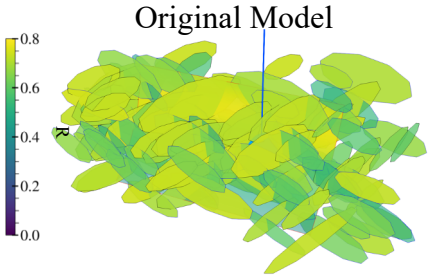

Injecting fluid directly into a permeable core of the main fault (P_f = 6 MPa).

- Rupture starts on main fault, propagates bilaterally, and then branches onto nearby fractures.
- Dynamic triggering occurs once the rupture on main fault reaches the edge of the main fault plane.
- Cascading earthquake occurs once the propagating rupture impinges on neighboring fractures.

Dynamic Rupture Earthquake Scenario 2

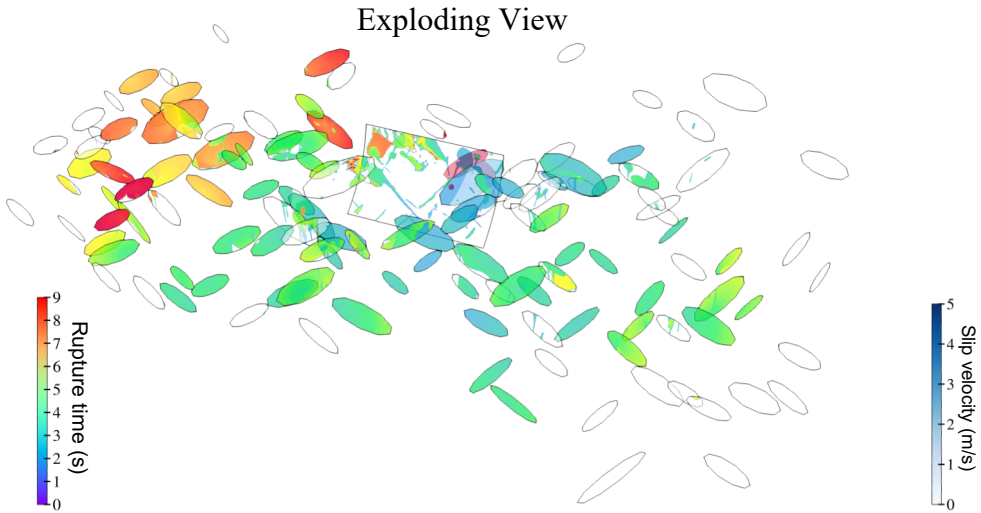

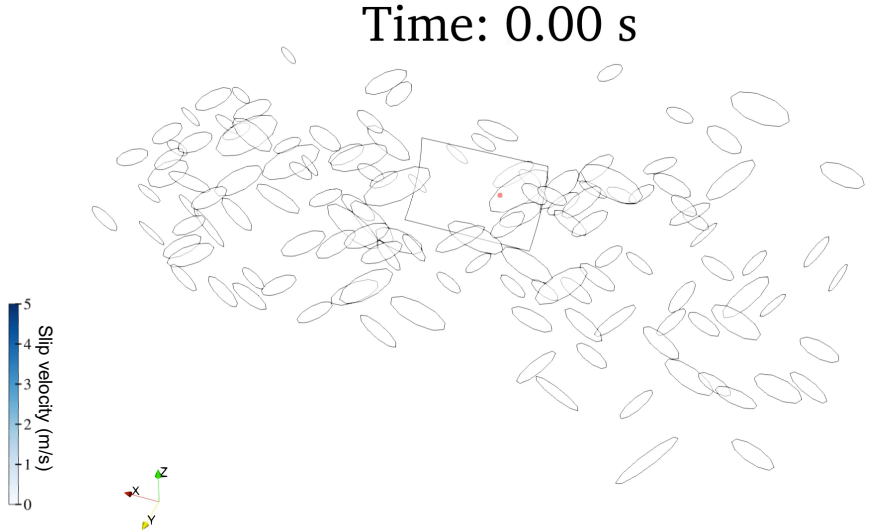

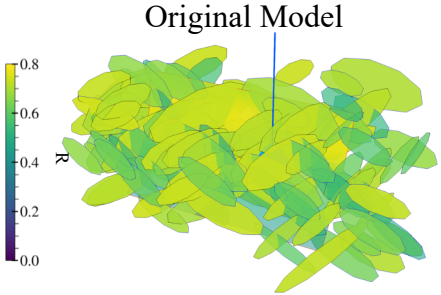

Injecting fluid into a volume of perturbing stress on the main fault and distributed fracture network (P_f = 4 MPa).

- Rupture propagates on fractures without triggering rupture on the main fault.
- Rupture evolves to intersected fractures creating cascading rupture to the fracture network.
- Dynamic interaction, fractures and the main fault, initiates rupture on the main fault but only produces multiple self-arrested rupture.

Dynamic Rupture Earthquake Scenario 3

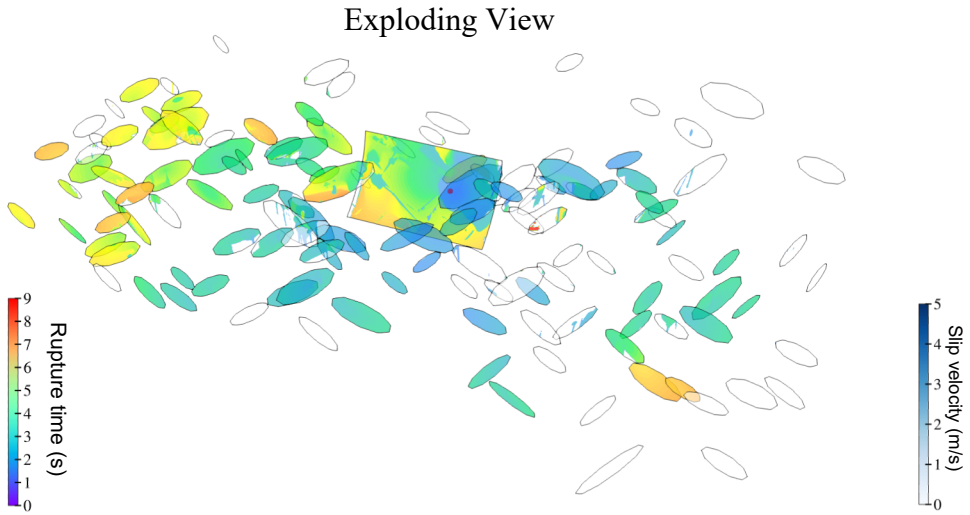

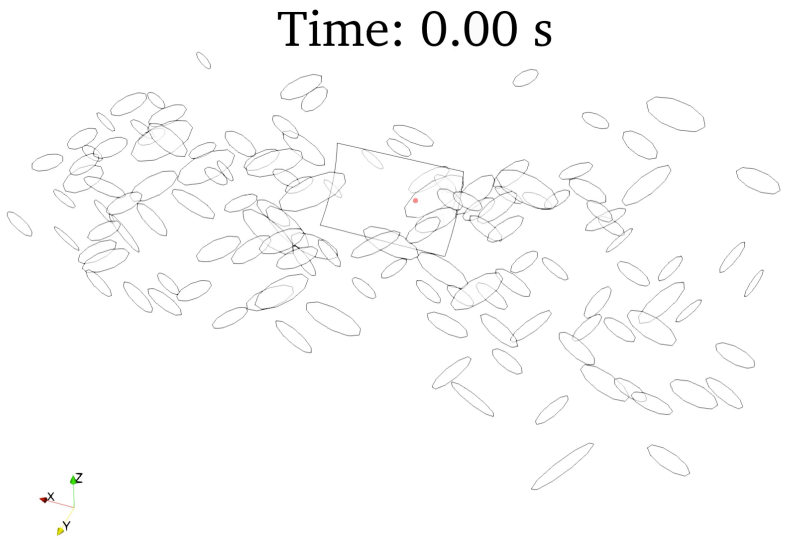

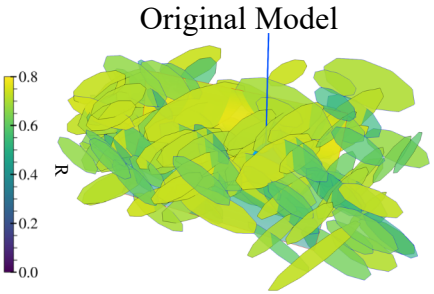

Same as S2, but stronger stress perturbation (P_f = 7 MPa).

- Rupture starts on the main fault and fracture network. Rupture on the main fault propagates unilaterally, activating fractures, and initiates cascading earthquake.
- At t = 2.5 s, the main fault re-nucleated, generating self-sustained rupture.

Summary of Source Properties

Scenario	Moment tensor solution	Overall moment magnitude	Ratio of rupture speed to shear wave speed	Average slip (m)	Average dynamic stress drop (MPa)
S1		6.36	0.88	0.17	7.1
S2		6.37	0.87	0.12	6.8
S3		6.39	0.86	0.16	7.6

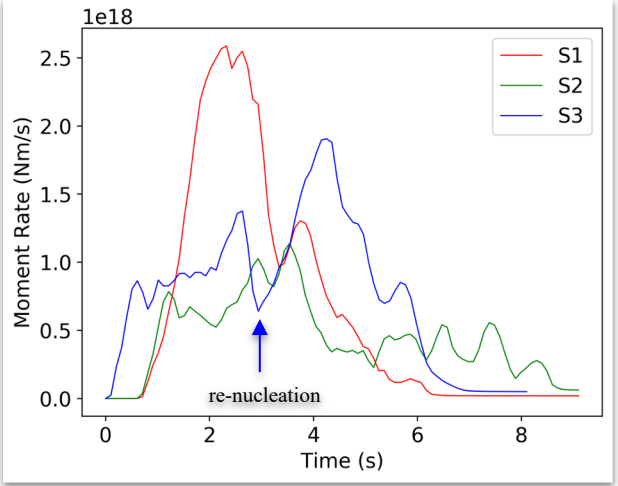

- Scenario 1 (S1): stress/strength perturbation along the main fault only (e.g. injection into a permeable fault core).
- Scenario 2 (S2): stress/strength perturbation into a rock volume spanning a subset of fractures and part of the main fault (e.g. injection into a fracture system within the fault damaged zone).
- Scenario 3 (S3): like S2, but larger stress perturbation.

❑ Moment rate function becomes higher when rupture on the main fault start to evolve, especially for S1 and S3 after re-nucleation.

Comparison to Observational Data

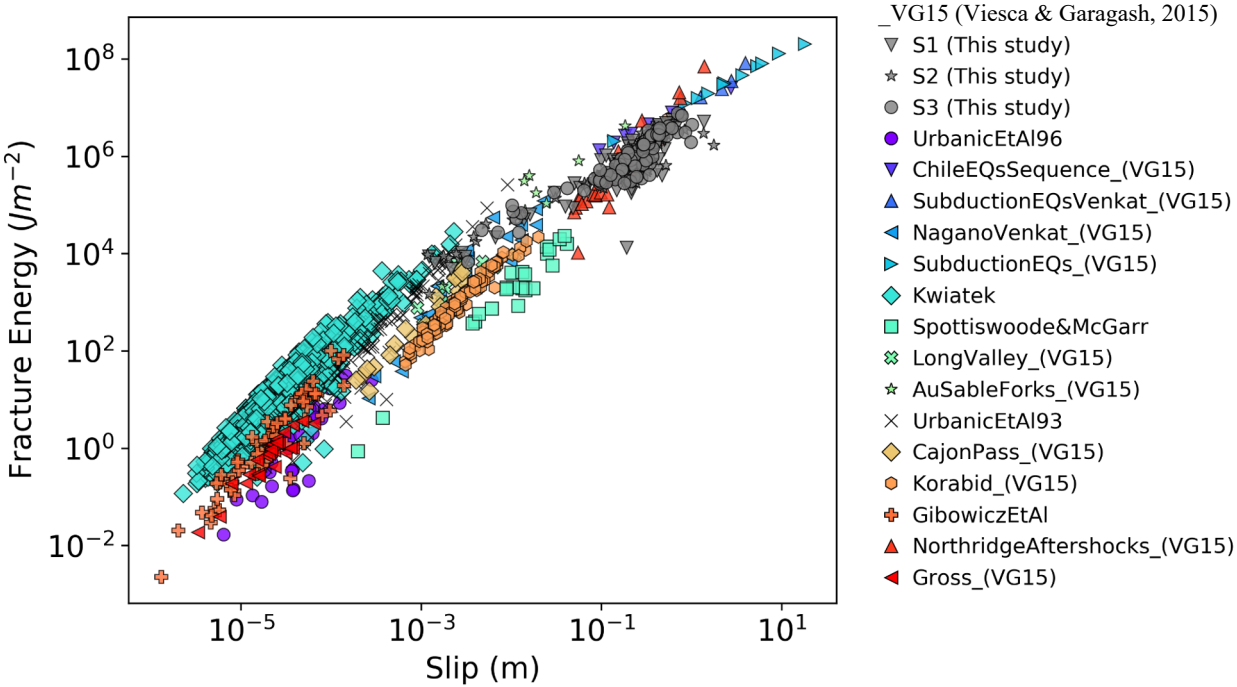

- All scenarios produce comparable fracture energy with respect to slip to observation data.

Key findings

- Fractures oriented favorably with respect to regional stress, connected fractures, and close to critically stressed fractures host a cascading earthquake with or without run-away rupture on the main fault.
- Cascading rupture with (scenario 1 and scenario 3) and without run-away rupture (scenario 2) on the main fault produce different moment tensor solutions. Surprisingly, scenario 2 results double-couple moment tensor solution.
- Cascading rupture in this study produce sub-rayleigh rupture speed and plausible fracture energy in comparison to observation data.
- The ongoing work explores the transition in the rupture mode from the rupture cascading over a fracture network to the rupture on the main fault only with change in the regional stress orientation… stay tuned….

References

Gabriel, A. A., Li, D., Chiocchetti, S., Tavelli, M., Peshkov, I., Romenski, E., & Dumbser, M. (2021). A unified first-order hyperbolic model for nonlinear dynamic rupture processes in diffuse fracture zones. *Philosophical Transactions of the Royal Society A*, *379*(2196), 20200130.

Garagash, D. I. (2021). Fracture mechanics of rate-and-state faults and fluid injection induced slip. *Philosophical Transactions of the Royal Society A*, *379*(2196), 20200129.

Holdsworth, R. E., Trice, R., Hardman, K., McCaffrey, K. J. W., Morton, A., Frei, D., ... & Rogers, S. (2020). The nature and age of basement host rocks and fissure fills in the Lancaster field fractured reservoir, West of Shetland. *Journal of the Geological Society*, *177*(5), 1057-1073.

Mitchell, T. M., & Faulkner, D. R. (2009). The nature and origin of off-fault damage surrounding strike-slip fault zones with a wide range of displacements: A field study from the Atacama fault system, northern Chile. *Journal of Structural Geology*, *31*(8), 802-816.

Okubo, K., Bhat, H. S., Rougier, E., Marty, S., Schubnel, A., Lei, Z., ... & Klinger, Y. (2019). Dynamics, radiation, and overall energy budget of earthquake rupture with coseismic off-fault damage. *Journal of Geophysical Research: Solid Earth*, *124*(11), 11771-11801.

Savage, H. M., & Brodsky, E. E. (2011). Collateral damage: Evolution with displacement of fracture distribution and secondary fault strands in fault damage zones. *Journal of Geophysical Research: Solid Earth*, *116*(B3).

Schultz, R., Skoumal, R. J., Brudzinski, M. R., Eaton, D., Baptie, B., & Ellsworth, W. (2020). Hydraulic fracturing-induced seismicity. *Reviews of Geophysics*, *58*(3), e2019RG000695.

Torabi, A., Johannessen, M. U., & Ellingsen, T. S. S. (2019). Fault core thickness: Insights from siliciclastic and carbonate rocks. *Geofluids*, *2019*.

Viesca, R. C., & Garagash, D. (2012, December). Steady slip pulses on faults with rate-and state-dependent friction and multiple thermal weakening mechanisms. In *AGU Fall Meeting Abstracts* (Vol. 2012, pp. S21B-2435).

Viesca, R. C., & Garagash, D. I. (2015). Ubiquitous weakening of faults due to thermal pressurization. *Nature Geoscience*, *8*(11), 875-879.

Wang, R., Gu, Y. J., Schultz, R., & Chen, Y. (2018). Faults and non-double-couple components for induced earthquakes. *Geophysical Research Letters*, *45*(17), 8966-8975.

Zhang, H., Eaton, D. W., Li, G., Liu, Y., & Harrington, R. M. (2016). Discriminating induced seismicity from natural earthquakes using moment tensors and source spectra. *Journal of Geophysical Research: Solid Earth*, *121*(2), 972-993.